ISSN 1063-7397, Russian Microelectronics, 2014, Vol. 43, No. 1, pp. 15–20. © Pleiades Publishing, Ltd., 2014.
Original Russian Text © I.I. Bobrinetskii, V.K. Nevolin, K.A. Tsarik, A.A. Chudinov, 2014, published in Mikroelektronika, 2014, Vol. 43, No. 1, pp. 23–28.

A Distribution of Ga^+ Ions in a Silicon Substrate for Nano-Dimensional Masking

I. I. Bobrinetskii, V. K. Nevolin, K. A. Tsarik, and A. A. Chudinov

National Research Institute MIET, Moscow, Russia

e-mail: vkn@miee.ru

Received June 25, 2013

Abstract—A nano-dimensional doping method of near-surface silicon layers using the focused ion beam was studied by software tools based on mathematical calculations of ion ranges in crystals. The sizes of local doping regions and concentrations of impurity atoms as function of real process parameters of the nano-dimensional exposure to the ion gallium beam are calculated. Theoretical boundaries of process doping parameters, taking silicon sputtering into consideration are determined.

DOI: 10.1134/S1063739713060036

INTRODUCTION

The focused ion-beam (FIB) lithography is one of the basic methods for creating nano-dimensional patterns with a resolution up to 10 nm, having found applications for designing different units and elements. The output of this method is low, restricting commercial use of this technology. The FIB is basically used for the reconstruction of photomasks for EUV lithography and creation of master-dies for nanoimprint lithography (NIL).

One of the new lithography methods uses gallium for forming masks directly on silicon [1]. By using the FIB it is possible to form nano-dimensional gallium-doped regions in the near-surface silicon substrate layer, forming specified patterns of required elements. The advantages of nano-dimensional ion doping enable us to obtain precision formations of profiles of semiconductor instrument structures due to the possibility of controlling the precision dose by changing the exposure time and accelerating voltage. Similar control accuracy ensures the high resolution of the formed mask (~40 nm) without recourse to a polymer for pattern transfer [2]. The high efficiency of focused ion beam systems enables a high throughput of the nanolithography process in electronics. The combination of the doping process and other manufacturing crystal surface treatment processes and the capability of creating virtually any distribution profiles due to step doping open broad prospects for this technology, e.g., when 3D patterns are formed by volumetric masking. The removal of these masks is a labor-consuming problem since gallium atoms are implanted into silicon, and destruction and changes caused by implanted ions in silicon have not been sufficiently studied.

A great number of regulating parameters of the ion-doping process (dose, type, ion energy, etc.) allows one within wide limits to change the properties of the doped layers but, along with this fact, requires a deep physical understanding of ion implantation processes, their behavior in the crystal lattice, the kinetics of the formation and elimination of radiation-induced defects, being necessary for high-quality technological modeling and the final efficient implementation of instrument structures and integrated circuits.

The characteristics of gallium ion implantation in silicon for creating a nano-dimensional topological pattern were studied theoretically in this work. Ion implantation parameters are necessary for evaluating etching rates and determining nanostructure sizes.

THE Ga^+ ION DOPING MODEL OF THE SILICON SUBSTRATE

The standard microelectronic technology implies semiconductor doping with impurities for creating different instrument structures by changing its electrophysical properties (type of electrical conduction, specific resistance, and other characteristics). However, local ion doping opens a possibility of forming a three-dimensional nano-dimensional pattern by combining FIB and plasma-chemical etching (PCE) technologies. Due to the difference in the etching rates of doped and undoped silicon regions, a three-dimensional object is formed on silicon by the PCE technology.

The formed 3D nano-dimensional pattern can be used, e.g., as a die for nanoimprint lithography. The sequence of nanostructure formation by FIB masking is as follows. The FIB lithography forms on the silicon surface a pattern, consisting of locally doped regions, which are further used as a mask for plasma-chemical etching (PCE) (Fig. 1).

A possible reason why the plasma-chemical etching of silicon regions doped with Ga^+ ions occurs much slower than that of "pure" regions lies in the

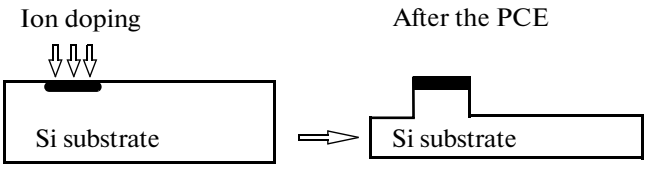

Fig. 1. The die formation scheme using the plasma-chemical etching of the silicon region doped with gallium ions.

Ga^+ ion compounds with oxygen and fluorine atoms, formed due to the PCE in plasma SF_6/O_2 [1].

The calculation of the parameters of the implanted ions was performed by the Monte Carlo simulation method. This method is clearly described in [3]. This method uses the binary collision approximation; i.e., it assumes that the probability of simultaneous collisions of three particles at one point of space is negligibly small.

A great number of paths of implanted particles were calculated in this work. The calculation for each particle started with the generation of a random position within the doping region, specifying the motion direction and energy E_0. We assume in the calculations that the particle travels in straight lines and changes its direction due to collisions. Penetrating into the crystal lattice, the ionized atom gradually loses the kinetic energy acquired by acceleration in the ionic column due to interactions with electrons and elastic collisions with semiconductor and impurity atoms, i.e., due to electron and nuclear deceleration. The calculation of particle motion stopped if its energy became smaller than a certain value, $E_{\min}$, or if the particle left the simulation region.

Let us introduce the following system of coordinates to calculate parameters of the gallium ion range in silicon. Let us direct the x axis perpendicular to the target surface, and the y and z axes along the surface perpendicular to one another. The path of the implanted ion up to the complete stop is a broken line and characterizes its range. One of the basic parameters of the ion range is the range projection in the direction of the initial motion path (the projective range (R_p)) and the projection on the y axis (the lateral range (R_{lat})).

The implantation of gallium ions during FIB operations into the silicon substrate without the material sputtering effect can be only with a small exposure dose, which is determined from parameters such as the ion beam current and exposure time at a point. Hence, the expression for the dose is written as

$$D = \frac{4It}{\pi d^2} n, \tag{1}$$

where I is the beam current, t is the exposure time, d is the beam diameter, and n is the number of passes.

The basic index of the ion implantation is the average path; i.e., the distance, which the implanted ion passes in the solid body up to the complete stop. This index mostly depends on the ion energy.

The Lindhard–Sharf–Shiott (LSS) theory was used to determine the average range. It helped to describe the penetration depth and spatial distribution of ions in amorphous bodies. In this respect, we assume that the ion, penetrated in the solid body, necessarily experiences collisions with the bound electrons and atomic nuclei of the substrate up to its complete stop. If the energy loss per unit length is taken into account, one can write the following expression for the energy loss:

$$\frac{dE}{dx} = \left(\frac{dE}{dx}\right)_{\text{nuclear}} + \left(\frac{dE}{dx}\right)_{\text{electron}}. \tag{2}$$

This expression is also written as:

$$-\frac{dE}{dx} = N_0\left[S_n(E) + S_e(E)\right], \tag{3}$$

where N_0 is the number of scattering centers in the volume unit; i.e., the atomic density (atom/cm^3); $S_n(E)$, and $S_e(E)$ are the nuclear and electronic decelerating abilities.

Then, the average range can be written as

$$\overline{R} = \int_0^R dx = \int_0^{E_0} \frac{dE}{\left(-\frac{dE}{dx}\right)} = \frac{1}{N_0}\int_0^{E_0} \frac{dE}{S_n(E) + S_e(E)}. \tag{4}$$

CALCULATION OF THE Ga^+ ION RANGE IN THE SUBSTRATE

The SRIM (Stopping and Range of Ions in Matter) software program was used to calculate the average range. This software uses the LSS theory and Monte Carlo method for the calculations. The initial parameters of the silicon substrate were specified. The bounded region at a depth of 990 Å and natural oxide on a 10 Å thickness surface were studied. The implantation of gallium ions with energies up to 30 keV was considered.

The simulation results of the propagation of gallium ions in the silicon body in the xy plane (the y axis corresponds to the surface level) is shown in Fig. 2.

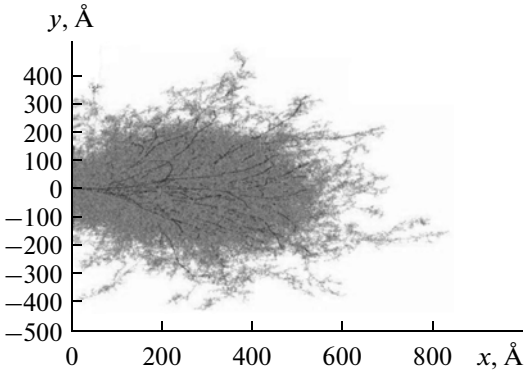

Fig. 2. Tree of paths of implanted ions and defects created in the target.

The availability of the natural silicon oxide insignificantly influences the ion range, since its thickness is sufficiently small, and the high vacuum of the ion beam system prevents it from growing further. As can be seen from the figure, the braking path of gallium ion can reach 80 nm in the substrate depth, but the main part of the ions is still held in a region from 5 to 60 nm in depth.

The dependence on the energy of the gallium ion was plotted to evaluate the projective and lateral ranges. The simulation results show the virtually linear dependence of the average projective ion range on the energy in an energy range up to 30 keV. Thus, the average thickness value of the doped layer (longitudinal component of the range) is determined by the ion acceleration and reaches 27 nm at 30 keV. The depth value, where the peak of the implanted ion concentration is located, coincides with the average projective ion range. The width of the doped region under the point action (lateral component of the range) changes weakly as the ion acceleration is increased. However, as can be seen from Fig. 3b, the contribution to the lateral displacement gives a 5-nm lateral range at 30 keV.

In the real case, it is insufficient to evaluate the average value. It is necessary to determine the deviation from the average value. Let us consider the deviation from the average value of the projective range along the longitudinal deviation reaching the projective range value. It is the same for the lateral range. The real depth of occurrence of the silicon-implanted ion, consisting of the projective range and longitudinal deviation, with an energy of 30 keV will vary from 30 to 60 nm. When the exposure is a point, the real diameter of the implanted ion location region is composed of the doubled sum of the average lateral range and its lateral deviation. The lateral deviation of the lateral range value, as the lateral range itself, is not less than 5 nm for silicon. The diameter of the ion location region with an energy of 30 keV is not less than 20 nm.

However, in the real case, it is necessary to add the ion beam diameter to this value. Thus, e.g., under the point action of a 7-nm diameter ion beam, according to the calculations, the doped region will have a diameter of 27 nm; i.e., it is necessary to use the ion beam diameter, the average projective range, and the average lateral range to calculate the geometrical parameters of the doped region. The radius of the ion beam or the radius of its focusing depends on the selected doping aperture. For example, aperture holes of 3.5, 6, 8, 9.5, 11.5, 16.5, 19.5, 25, and 40.5 nanometers are more often used for FEI devices. They correspond to beam current values of 0.001, 0.01, 0.03, 0.05, 0.1, 0.3, 0.5, 1, and 3 nA.

The thickness of the doped region h does not depend on the selected aperture but is determined by the doping dose and, as was shown above, the initial beam energy. In order to study the ion concentration distribution, the gallium ion distribution profile in the

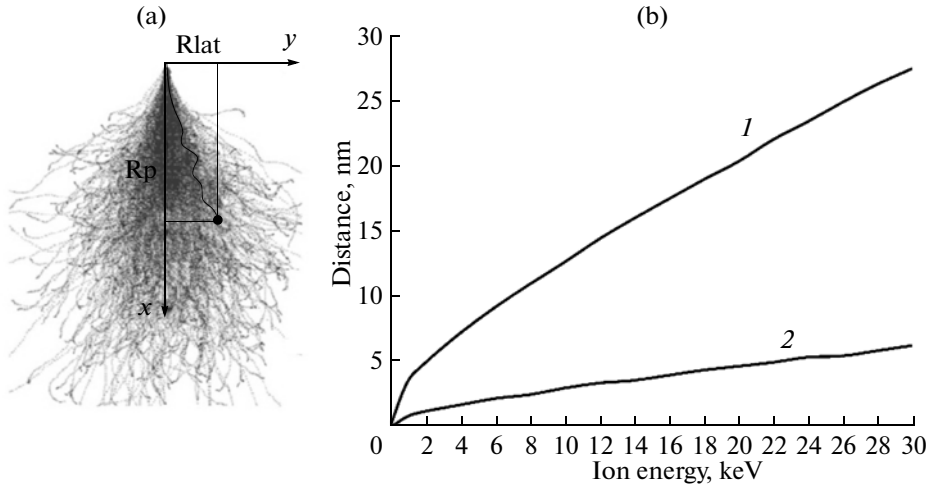

Fig. 3. (a) Schematic drawing of the basic parameters of the ion range in the solid body, and (b) simulation result of the (*1*) average ion range projected on the direction of the movement and (*2*) lateral range.

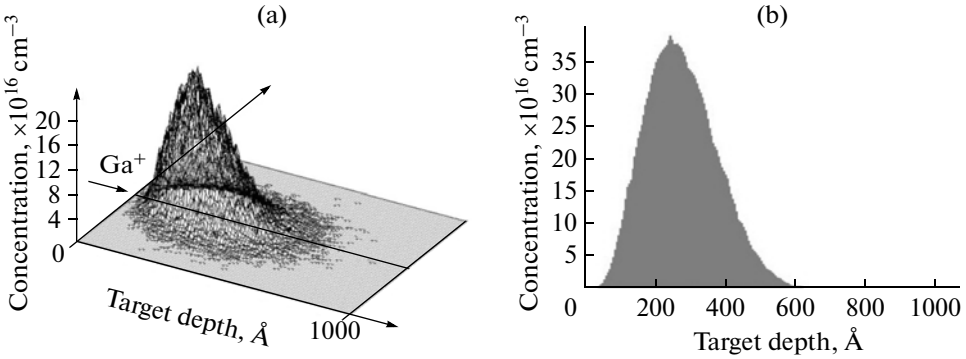

Fig. 4. (a) Image of three-dimensional distribution and (b) distribution profile of Ga^+ ions in the silicon substrate with an exposure ion dose of 1×10^{12} cm^{-2}.

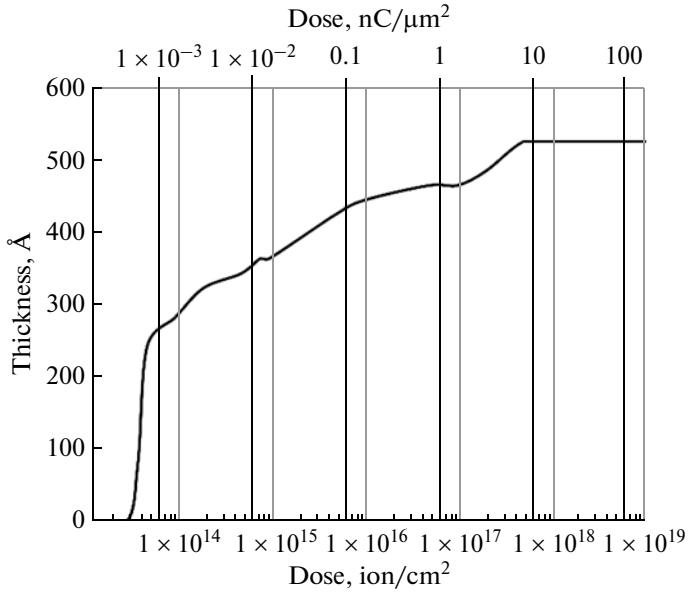

Fig. 5. Dependence of the thickness of the damaged layer on the ion implantation dose.

silicon substrate is simulated and plotted. Figure 4 shows the profile image obtained from the simulation results in the SRIM. This program uses the Monte Carlo method for calculating ion paths. The specified values of the basic parameters of the ion beam exposure are as follows: the ion beam energy is 30 keV, and the acting ion dose is 1×10^{12} cm^{-2} for a current beam of 30 pA and beam diameter of 16 nm. In the figure, the arrow shows the place of the ion beam exposure. It can be seen that the maximum is in the implanted ion concentration distribution in depth. The concentration is at the minimum at surface level. The gallium atom occurrence range reaches 70 nm. However, the maximum doping level is not on the surface but at a depth of about 30 nm. The main part of ions, the concentration of which is not smaller than 5×10^{16} cm^{-2}, is packed into a region of 10- to 50-nm depth. The peak concentration was 4×10^{17} cm^{-2}.

AMORPHIZATION OF THE SUBSTRATE IN THE PROCESS OF Ga^+ ION IMPLANTATION

In order to take into account the silicon amorphization and sputtering effects in the doping process, one should take into account the impurity concentration. If the ion concentration in silicon exceeds the solubility limit of 4×10^{19} cm^{-3} [4], the crystal lattice collapses. Thus, when exposure doses of the ion beam are large, the amorphous domain in the near-surface crystal region is formed; i.e., in the case shown in Fig. 4, silicon is not damaged, since the doping level is not exceeded. Based on the simulation data in the 2DIonMonterCarlo software, which allows one to evaluate the damage of the crystal lattice, the dependence of the response of the dose of the acting ion beam dse on the amorphous domain value that is formed until the etching well starts being formed was

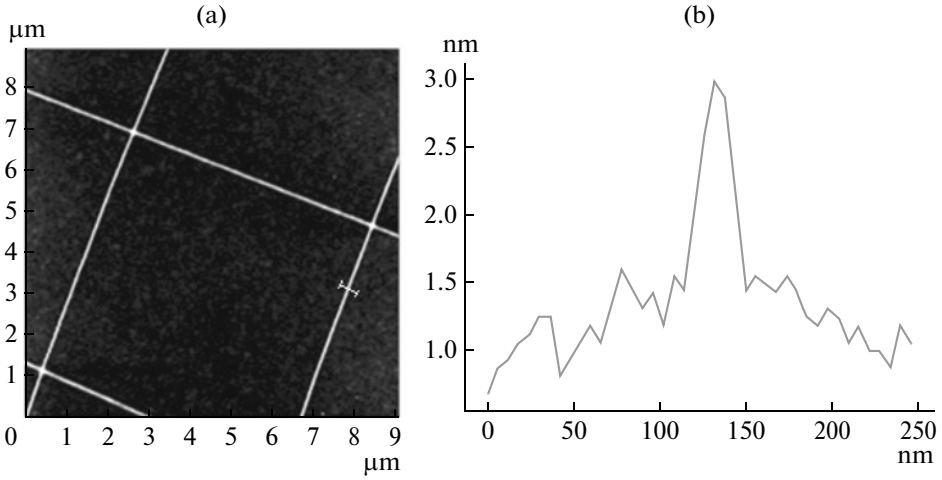

Fig. 6. (a) AFM image of the structure obtained by the PCE and (b) cross section of one of strips of this structure.

obtained. The thickness of the amorphous layer was determined by the borders of the 100% damage of the crystal lattice.

The dose of exposure to the sample surface (see Fig. 5) significantly influences the thickness of the amorphous region. When the implantation dose is about 10 nC/μm^2, the amorphization is entirely supported at one level and located under the bottom of the ion-etched crater. This should be taken into account in calculations of the effective thickness of the masking region. The amorphous layer reaches its limit value of 51 nm, when the ion energy $E = 30$ keV and the acting ion dose is 2.5×10^{17} cm^{-2} or 0.04 nC/μm^2. When the ion beam density is 88.42 nA/μm^2 and the beam diameter is 7 nm, under an exposure dose of 0.03 nC/μm^2 the silicon substrate's etching depth corresponds to 2 nm and the width is about 23 nm, (see [5]).

Thus, of the calculated 51 nm of the damaged region, 2–3 nm near the surface correspond to the etched well depth. When the ion beam exposure dose is 1.5×10^{14} cm^{-2} or 2.5×10^{-5} nC/μm^{-2}, the damaged region's depth coincides with the longitudinal ion range value (projection of the ion range on the moving direction).

EXPERIMENTAL STUDY OF PATTERN FORMATIONS DURING MASKING BY Ga^+ IONS

Based on the ion distribution calculation, the silicon sample was locally doped by exposure to the surface by the focused Ga^+ ion beam. The ion beam's parameters were specified, namely, the beam energy was 30 keV, the beam current was 10 pA, the beam diameter was 12 nm, and the implanted dose was 10^{12} cm^{-2}. The exposure was performed using a grid consisting of ten horizontal and ten vertical lines spaced 6.25 μm apart. The sample was subjected to the subsequent plasma-chemical etching in plasma SF_6/O_2. The silicon sample was scanned by the atomic-force microscope (AFM). Figure 6 shows the AFM image and the profile of the obtained structures. The width of the lines extending over the surface was 30 nm, coinciding with the calculation data. The height of the structures indicates that the formed mask does not restrain the PCE for a long time. However, the problem of obtaining the maximum height of the structures was not on the agenda. It is important to note that the lines' brightness increases at crosses in Fig. 6a, pointing to the increase in the structure's height on the AFM image. This feature indicates the strengthening of the masking effect as the impurity concentration is increased.

CONCLUSIONS

The performed theoretical studies enabled us to calculate doping parameters for creating nano-dimensional electronic elements by the focused-ion-beam doping procedure. The ion implantation simulation visually showed the region of their occurrence. The upper bound limiting the ion implantation dose is determined by the doped layer thickness, connected with the amorphization depth of the structure. In this case, the silicon doping depth will be equal to the deviation of the longitudinal range, which can be equal to the longitudinal range value. The doping region's width, specifying the topological sizes of the minimal elements, according to the calculations, will be 27 nm for the case when the ion beam density is equal to 88.42 nA/μm^2 and the beam diameter is 7 nm. In this case, as the experiment shows, it is possible to form masks for creating nano-dimensional topological elements with a width of about 30 nm. In this case, as the ion implantation dose is increased simultaneously with the increase in the thickness of the amorphous

layer, the masking is strengthened due to plasma-chemical etching.

ACKNOWLEDGMENTS

This work was supported by the Federal Targeted Program "Human Capital for Science and Education in Innovative Russia" for 2009–2013, project no. 14.V37.21.0064.

REFERENCES

1. Chekurov, N., Grigoras, K., Peltonen, A., Franssila, S., and Tittonen, I., The fabrication of silicon nanostructures by local gallium implantation and cryogenic deep reactive ion etching, *Nanotechnology,* 2009, vol. 20, no. 6, p. 065307-1.
2. Shearn, M., Sun, X., David Henry, M., Yariv, A., and Scherer, A., Advanced plasma processing: etching, deposition and wafer bonding techniques for semiconductor applications, *Semiconductor Technologies: Etching in Tech.,* 2010, Ch. 5, p. 79.
3. Nikonenko, V.A., *Matematicheskoe modelirovanie tekhnologicheskikh protsessov: Modelirovanie v srede MathCAD. Praktikum* (Mathematical Modeling of Manufacturing Processes: Simulation in the MathCAD Environment. Practical Work), Kuznetsov, G.D., Ed., Moscow: MISiS, 2001.
4. Wittman, R., Miniaturization problems in CMOS technology: Investigation of doping profiles and reliability, PhD thesis. Technische Universitat Wien, 2010. URL: http://www.iue.tuwien.ac.at/phd/wittmann/diss.html (application data 31.05.2013).
5. Bessonova, A.V., Nevolin, V.K., Romashkin, A.V., and Tsarik, K.A., Systematic features of the formation of semiconductor nanostructures using a focused ion beam, *Semiconductors*, 2012, vol. 46, no. 13, p. 1604.

Translated by N. Pakhomova